Biosensors and Bioelectronics 81 (2016) 423–430

Contents lists available at ScienceDirect

Biosensors and Bioelectronics

journal homepage: www.elsevier.com/locate/bios

# Wavelength-resolved simultaneous photoelectrochemical bifunctional sensor on single interface: A newly in vitro approach for multiplexed DNA monitoring in cancer cells

Yingning Zheng [a], Wenbin Liang [a,b], Yali Yuan [a], Chengyi Xiong [a], Shunbi Xie [a], Haijun Wang [a], Yaqin Chai [a,*], Ruo Yuan [a,*]

[a] Education Ministry Key Laboratory on Luminescence and Real-Time Analysis, College of Chemistry and Chemical Engineering, Southwest University, Chongqing 400715, People's Republic of China

[b] Department of Clinical Biochemistry, Laboratory Sciences, Southwest Hospital, Third Military Medical University, 30 Gaotanyan Street, Shapingba District, Chongqing 400038, People's Republic of China

ARTICLE INFO

*Article history:*
Received 1 February 2016
Received in revised form
5 March 2016
Accepted 14 March 2016
Available online 15 March 2016

*Keywords:*
Photoelectrochemical biosensor
Single interface
Multiplexed detection
Cell
Signal amplification

ABSTRACT

Currently, the photoelectrochemical (PEC) strategies can just achieve single analyte detection on a single interface with limited detection efficiency. It is highly valuable but full of challenge to develop a PEC biosensor for multiple analytes evaluation on a single interface. For this point, the wavelength-selective photoactive materials, which could generate separated photocurrents under excitation lights with certain wavelengths, were mainly important to overcome this challenge. Herein, these wavelength-selective photoactive materials were successfully synthesized and served as signal indicators to construct a novel PEC biosensor for multiple analytes evaluation on a single interface for the first time. Moreover, an enzyme-assisted target recycling amplification strategy was introduced for ultrasensitive monitoring. As a result, the proposed PEC biosensor showed excellent analytical performance for both oral cancer (ORVOA 1) gene and p53 gene down to attomolar level. In addition, the fabricated PEC biosensor was employed to evaluate ORVOA 1 gene and p53 gene in Hela cells. This assay has laid the foundation for fabrication of simple, ultrasensitive and economical PEC diagnostic devices to detect multiple analytes in cells, which paved a new avenue for early diagnosis of cancer with higher efficiency and accuracy.

© 2016 Elsevier B.V. All rights reserved.

## 1. Introduction

The development of assays to quantify multiplexed nucleic acid sequences, proteins or cells in a highly-efficient, selective and sensitive fashion has been one of the major goals in practical bioanalysis, especially clinical diagnostics. (Li et al., 2016; Pal et al., 2015; Zhu et al., 2014) Compared with traditional assays, the multiplexed assay possesses higher-throughput, higher detection efficiency, simpler analytical process and lower cost. (Lee-Montiel et al., 2015) Up to now, some multiplexed detection strategies with traditional fluorescent or electrochemical detection techniques have been successfully constructed, which depend on the targets labeled with fluorophores or redox probes with different excitation/emission wavelengths or oxidation/reduction potentials. (Pepperkok et al., 1999; Yang et al., 2015; Lee et al., 2007; Hansen et al., 2006) Although these established technologies are advantageous for high-throughput detection and easy labeling, improvements are still required since their limitations on sensitivity and accuracy. The photoelectrochemical (PEC) assay as a newly developed analytical technique has significant advantages over the traditional optical and electrochemical methods such as lower background, higher sensitivity, better accuracy and lower cost. (Ge et al., 2013, 2015; Yu et al., 2015; Zhao et al., 2014; Wang et al., 2014; Shen et al., 2014; Zhuang et al., 2015; Shu et al., 2015) Recently, Hu's group reported a PEC biosensor for multiple biomarkers assay on a single electrode by a light addressing strategy. (Hu et al., 2015) The multiplexed detection by PEC strategy was accomplished by dividing the electrode into different interfaces for capturing different targets, followed with a moving light source to scan each interfaces on the electrode. Although a higher detection efficiency can be obtained with this strategy, some limitations still existed for further improvement. First, the fabrication process of the biosensor was tedious and time-consuming by dividing a single electrode into different interfaces. More importantly, it's hard to divide the electrode into different interfaces evenly. Second, the light addressing strategy requires tough operations for equipment. Besides, it is hard to irradiate each section of the

* Corresponding authors.
*E-mail addresses:* yaqinchai@swu.edu.cn (Y. Chai), yuanruo@swu.edu.cn (R. Yuan).

http://dx.doi.org/10.1016/j.bios.2016.03.032
0956-5663/© 2016 Elsevier B.V. All rights reserved.

electrode evenly. The sensitivity, accuracy and reproducibility of the fabricated biosensor would be decreased due to these limitations. To overcome these limitations, the multiplexed PEC assay on single interface, which possessed more simple operations, higher accuracy and sensitivity than the multiplexed assay on different interfaces, was highly desired to improve the detection efficiency and simplify the analytical process.

The major challenge for realizing the multiplexed PEC assay on single interface is to generate distinct signals for each target in one test sample. To address this challenge, different wavelength-selective photoactive materials, which could generate separated photocurrents under excitation lights with certain wavelengths, should be synthesized and served as signal indicators for the different targets in detection of these multiplexed targets. In addition, there should be no energy transfer among these wavelength-selective photoactive materials. For this point, we recently explored the photocurrents of varies photoactive materials under excitation lights with different wavelengths to search the desirable wavelength-selective photoactive materials. Consequently, we have found the multi-wall carbon nanotube (MWCNT)/ poly (ethylenimine) (PEI)/ thionin (Thi) nanocomposite (MPT NPs) and the self-synthesized flower-in-sphere like $TiO_2$ nanoparticles ($TiO_2$ NPs) showed well wavelength selectivity under excitation lights of 590 nm and 365 nm, respectively. In addition, further experiments indicated that there was no energy transfer between the MPT NPs and $TiO_2$ NPs. Thus, the MPT NPs and $TiO_2$ NPs would be the optimum candidates to be served as signal indicators for the different targets in the multiplexed PEC assay on single interface.

The other challenge for achieving the multiplexed PEC assay on single interface was to overcome the limitation of low signal output. Typically, effective signal amplification strategies were employed to enhance the signal output for ultrasensitive detection. Herein, an enzyme-assisted target recycling amplification strategy was introduced to further improve the sensitivity of the fabricated PEC biosensor by employing the nicking endonuclease N.BstNB I enzyme which could selectively cleave only one strand of a double stranded DNA base away from the 3′-end of its recognition sequence (5′-GAGTC-3′). (Chen et al., 2013) The specific recognition effect of N.BstNB I enzyme made it more selective and sensitive than other DNA-based amplification strategies such as polymerase chain reaction, rolling circle amplification, hybridization chain reaction and exonuclease III-assisted target recycling strategy. (Palecek and Bartosik, 2012).

Herein, a novel multiplexed PEC assay on single interface was demonstrated for in vitro DNA monitoring with oral cancer (ORVOA 1) gene and p53 gene as model which were normally employed as efficient biomarkers for early diagnosis of cancer. (Yuan et al., 2015) As shown in Scheme 1, the multiplexed PEC sensing strategy was relied on the wavelength-selective photoactive materials MPT NPs and $TiO_2$ NPs to act as signal indicators for the target ORVOA 1 gene and p53 gene, respectively. Furthermore, the enzyme-assisted target recycling amplification can offer effective signal amplifications by cleaving the signal probes upon binding to the target to release and reuse the target. And the cleaved probes could be immobilized on the electrode by hybridizing with the capture DNA on the electrode surface, leading to a photocurrent response for target quantitative determination. Moreover, ORVOA 1 gene and p53 gene derived from curcumin induced Hela cells were employed to demonstrate the applicability of the fabricated PEC biosensor. The multiplexed PEC assay with the amplification technology for in vitro DNA monitoring on single interface opened a new horizon for highly efficient detection of nucleic acid sequences, proteins and cells in early diagnosis of cancers.

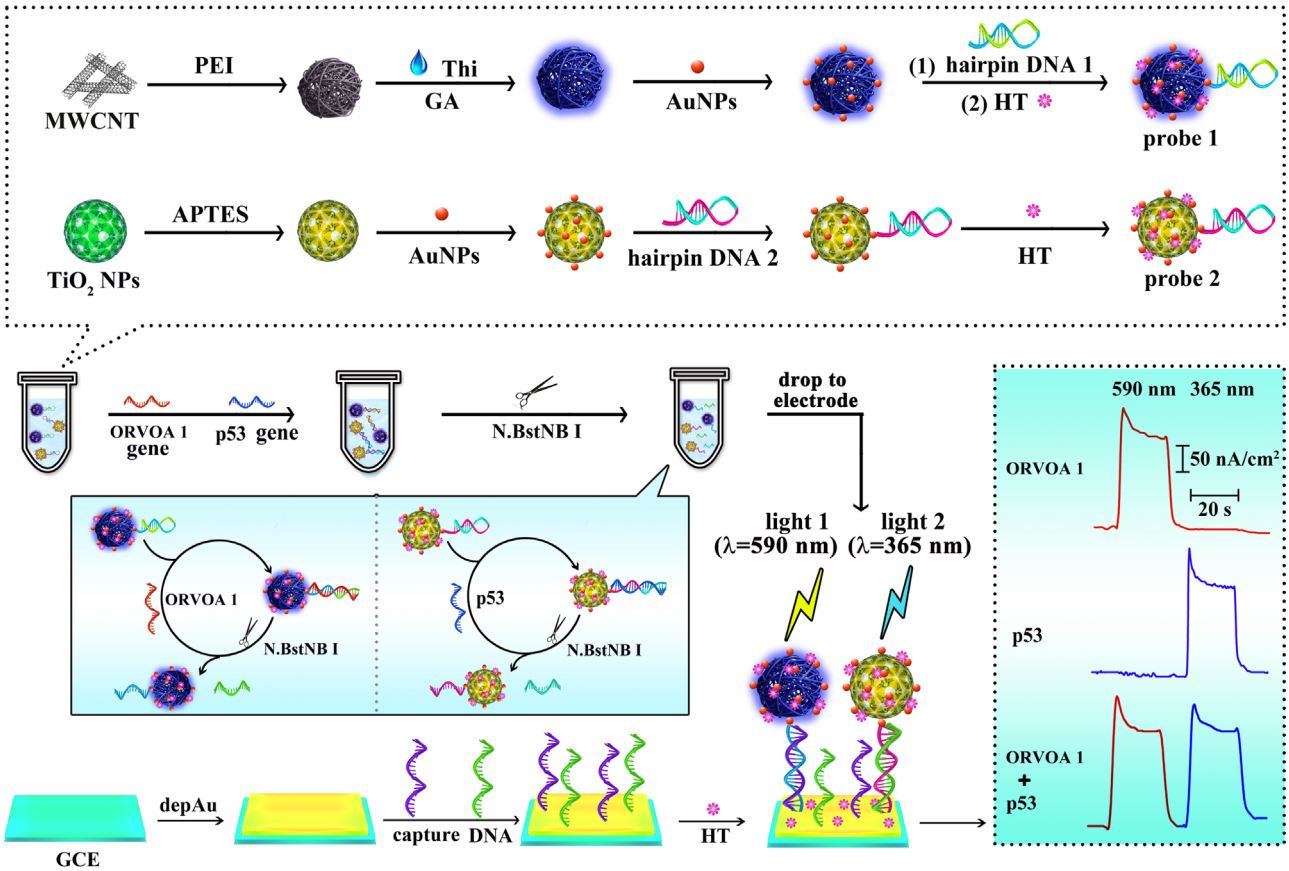


**Scheme 1.** Schematic diagram for the fabrication of the PEC biosensor.

## 2. Experiment

### 2.1. Chemicals and material

MWCNT was obtained from Nanjing Xianfeng Nano Materials Tech Co. Ltd. (Nanjing, China). PEI (average Mn ~ 10,000 by gel permeation chromatography, purity > 99%), thionin (Thi), glutaric dialdehyde (GA), gold chloride ($HAuCl_4$), (3-aminopropyl) triethoxysilane (APTES), hexanethiol (HT) and curcumin were purchased from Sigma-Aldrich (St. Louis, Mo, USA). The N.BstNB I enzyme and 10 × NEBuffer were obtained from New England Biolabs (Ipswich, USA). Sodium borohydride ($NaBH_4$), hydrogen peroxide ($H_2O_2$), tetrabutyl titanate and glacial acetic acid were purchased from Kelong Chemical Inc. (Chengdu, China). Gold nanoparticles (AuNPs) (16 nm diameter) were synthesized according to the literature. (Lee et al., 2009) Phosphate buffer solution (PBS) (pH 7.0) purchased from Beijing Dingguo Changsheng Biotechnology Co. Ltd. (Beijing, China) was used as the electrolyte throughout the photocurrent measurement. Ferricyanide/ferrocyanide solution ($[Fe(CN)_6]^{3-/4-}$, 5.0 mM) was obtained by dissolving potassium ferricyanide and potassium ferrocyanide with PBS (pH 7.4). Tris–HCl buffer (20 mM, pH 7.4) containing 140 mM NaCl, 5 mM KCl, 1 mM $CaCl_2$ and 1 mM $MgCl_2$ was used for preparing DNA solutions. The diethypyrocarbonate (DEPC)-treated water and 4′, 6-diamidino-2-phenylindole (DAPI) were obtained from Beyotime Institute of Biotechnology (Jiangsu, China). The Hela cell line was acquired from the cell bank of the Committee on Type Culture Collection of Chinese Academy of Science (Shanghai, China). The fetal bovine serum (FBS) was obtained from Hyclone (UT, USA). The penicillin and streptomycin were purchased from Thermo Fisher Scientific Inc. (Waltham, USA). The RNAprep pure cell/Bacteria Kit was purchased from TianGen Co., Ltd. (Beijing, China). The GoldStar TaqMan Mixture was obtained from Shanghai Sangon Biological Engineering Technology and Services Co., Ltd. (Shanghai, China). The aqueous solutions used in the experiment were prepared with ultrapure water.

All oligonucleotides were bought from Shanghai Sangon Biological Engineering Technology and Services Co., Ltd. (Shanghai, China). The details of these sequences were listed as following:

### 2.2. Apparatus and characterization

The PEC measurements were performed with a PEC workstation (Ivium, Netherlands). A conventional three-electrode system was used for photocurrent measurement, in which a platinum wire was served as the counter electrode, a saturated calomel electrode was served as the reference electrode and a bare or modified glassy carbon electrode (GCE) with 4 mm diameter was served as working electrode, respectively. Electrochemical impedance spectroscopy (EIS), cyclic voltammetry (CV) and electrochemical depositions were carried out with a CHI 660e electrochemical workstation (Shanghai Chenhua Instrument, China). The morphologies of the prepared nanomaterials were characterized by the scanning electron microscopy (SEM, S-4800, Hitachi, Japan). The light field microscope (LF) and fluorescence microscope (FL) measurements were performed by IX83 inverted fluorescence microscope (Olympus, Japan).

### 2.3. Synthesis of probe 1 (MPT NPs/AuNPs/hairpin DNA 1/HT) and probe 2 ($TiO_2$ NPs/AuNPs/hairpin DNA 2/HT) photoactive bionanoconjugates

The MPT NPs/AuNPs/hairpin DNA 1/HT photoactive bionanoconjugates (probe 1) were synthesized by modifying hairpin DNA 1 onto MPT NPs/AuNPs nanomaterials. Briefly, 2.0 mg carboxylated MWCNT was added into 4.0 mL ultrapure water with continuous ultrasonication to obtain a homogeneous solution. Then, 400 μL PEI solution (1%, *w*/*w*) was dropped into the mixture followed with continuous stirring for 12 h at room temperature to wrap the wire-like MWCNT into spherical MWCNT-PEI. Subsequently, 15 μL GA solution (5%, *w*/*w*) and 1 mL Thi solution (3 mM) were added into the mixture with continuous stirring for 50 min. After that, the prepared AuNPs solution (2 mL) was added and stirred for 16 h. The obtained solution was centrifugated to remove the unbounded AuNPs, and the precipitation was dispersed in 2 mL ultrapure water. Next, 25 μL hairpin DNA 1 solution (2.5 μM) was added to the mixture and stirred for 16 h at 4 °C. Consequently, 50 μL HT solution was dropped to the mixture and stirred for 40 min to block the nonspecific binding sites. Finally, the mixture solution was centrifuged to remove the excess reagents and the obtained precipitation (probe 1) was dispersed in 2 mL ultrapure water for further use.

In order to prepare the $TiO_2$ NPs/AuNPs/hairpin DNA 2/HT photoactive bionanoconjugates (probe 2), the $TiO_2$ NPs with flower-in-sphere nanostructure were synthesized firstly based on traditional method with some modifications. (Chen et al., 2015) Briefly, 10 mL tetrabutyl titanate was slowly added to 3.5 mL ethanol. The obtained mixture solution were stirred for 10 min to obtain solution A. At the same time, 0.4 mL glacial acetic acid and 1 mL ultrapure water were added to 3.5 mL ethanol with continuous stirring to obtain solution B. The pH value of solution B was adjusted to about 3 by HCl solution. Subsequently, the solution A was dropped into solution B with a speed of 3 mL/min under stirring. Then, the mixture solution was heated in 40 °C water bath for 2 h to a jelly-like mixture. The mixture was dried in vacuum drying oven at 70 °C overnight to obtain white $TiO_2$ particles. Finally, 0.2 g $TiO_2$ particles were dispersed in 10 mL ultrapure water and ultrasonicated for 2 days to obtain the $TiO_2$ NPs.

The $TiO_2$ NPs/AuNPs/hairpin DNA 2/HT photoactive bionanoconjugates (probe 2) were further prepared as followed. Firstly, 100 μL APTES solution was slowly dropped into the prepared 10 mL $TiO_2$ NPs solution under gently stirring. After 6 h stirring, the solution was filtered and washed respectively, and the precipitation was redispersed in 4 mL ultrapure water. Subsequently, 2 mL AuNPs solution was added into the above solution with stirring for 16 h. Then, 25 μL hairpin DNA 2 (2.5 μM) solution was added into the prepared $TiO_2$ NPs/AuNPs solution under gently stirring for 16 h at 4 °C. Next, 50 μL HT solution was added with stirring for 1 h to block the nonspecific binding sites. Finally, the mixture solution was centrifuged to remove the excess reagents and the obtained precipitation (probe 2) was redispersed in 2 mL ultrapure water for further use.

### 2.4. The procedure of N.BstNB I enzyme-assisted target recycling amplification strategy

Briefly, 7 μL probe 1 solution, 7 μL probe 2 solution, 3.2 μL 10 × NEBuffer, 7 μL ORVOA 1 gene solution and 7 μL p53 gene solution were added into a centrifuge tube. After gently stirring for 30 min, 1.0 μL N.BstNB I enzyme (10 U/μL) was added and incubated at 55 °C. Subsequently, the mixture was heated to 90 °C and kept for 10 min to deactivate the N.BstNB I enzyme. Finally, the mixture was cooled down to room temperature for further use.

### 2.5. Fabrication of the multiplexed PEC biosensor

Firstly, the GCE was polished with 0.3 μm and 0.05 μm $Al_2O_3$ powder and rinsed thoroughly with ultrapure water to obtain a mirror-like surface. Then the electrochemical deposition was performed in 1% $HAuCl_4$ solution under −0.2 V for 30 s to modify AuNPs onto the electrode surface. Next, the AuNPs modified electrode was dipped in the mixture solution containing 15 μL

capture DNA 1 (2.5 μM) and 15 μL capture DNA 2 (2.5 μM) for 14 h at room temperature. Finally, the electrode was dipped in HT solution for 40 min to block the nonspecific binding sites. After each step, the electrode was washed gently by ultrapure water to remove the unbonded reagents.

### 2.6. PEC measurement

Before photocurrent measurement, the solution of enzyme-assisted target recycling was ultrasonicated for few seconds to get a homogeneous solution. Then the homogeneous solution was dropped onto the fabricated electrode surface and incubated for 2 h at room temperature. Then the PEC measurement was carried out in 4 mL PBS (pH 7.0) containing 0.1 M freshly prepared $H_2O_2$ solution. The 590 nm and 365 nm excitation light sources were provided by the LED lamp and switched off-on-off for 10–20–10 s under 0.0 V potential.

### 2.7. Preparation of real samples from drug induced cancer cells

The Hela cell line was cultured in Dulbecco's Modified Eagle's Medium containing 10% FBS, 100 U/mL penicillin and 100 U/mL streptomycin in a humidified atmosphere with 5% $CO_2$ at 37 °C. The Hela cells with different expression of ORVOA 1 gene and p53 gene were obtained by incubating with different concentrations of curcumin (0, 5, 10, 20, 50, 100 μM) for 24 h. The curcumin induced Hela cells on 24 well-plates were stained with DAPI and viewed by the fluorescence microscope. For multiplexed detection of the ORVOA 1 gene and p53 gene in curcumin induced Hela cells, these Hela cells were extracted firstly using RNAprep pure Cell/Bacteria Kit according to the manufacturer's protocol, and followed by processing with reverse transcription-polymerase chain reaction (RT-PCR) technology with SGExcel GoldStar TaqMan Mixture on the basis of the manufacturer's protocol to obtain the corresponding DNAs. Then the corresponding DNAs were collected and stored at −20 °C for further use.

## 3. Results and discussion

### 3.1. Characterizations of the synthesized nanomaterials

The synthesized nanomaterials were characterized by SEM. As shown in Fig. 1 A, MWCNT showed tangled tubular structure with about 20 nm diameter. When wirelike molecular PEI was wrapped on the MWCNT, the structure of MWCNT was curved together due to the glutinosity of PEI (Fig. 1B). After the modification of AuNPs, some uniformly distributed AuNPs can be observed on the surface of the prepared nanomaterials (Fig. 1C). As shown in Fig. 1D, the proposed $TiO_2$ NPs showed an average particle size distribution of about 200 nm with flower-in-sphere nanostructure. After the decoration of AuNPs on the $TiO_2$ NPs, some small particles could be observed on the $TiO_2$ NPs (Fig. 1E), which was conducive to further modification. Furthermore, tyndall effect was employed to characterize the dispersivity and permeability of the synthesized $TiO_2$ NPs (a), $TiO_2$ NPs/ AuNPs (b), MWCNT (c), MWCNT/ PEI (d), MWCNT/ PEI/ Thi (e) and MWCNT/ PEI/ Thi/ AuNPs (f) (Fig. 1F). The obvious light-path indicated the good dispersivity and permeability of these synthesized nanomaterials in water.

### 3.2. Electrochemical characterizations for the stepwise fabrication of the PEC biosensor

The fabrication procedures of the PEC biosensor were characterized by EIS and CV measurements as showed in Fig. S-1. It was well known that the value of the electron-transfer resistance ($R_{et}$) of the electrode was an important factor for characterization of the electrode. Fig. S-1A showed the EIS of the different modified electrodes in 3 mL $[Fe(CN)_6]^{3-/4-}$ electrolyte solution (5 mM). There was a small semicircle for bare GCE ($R_{et} \approx 280\ \Omega$) (Fig. S-1A, curve a). When AuNPs were deposited on the electrode, the resistance decreased largely ($R_{et} \approx 17\ \Omega$) (Fig. S-1A, curve b) due to the good conductivity of the AuNPs. After capture DNA 1 and capture DNA 2 were immobilized on the modified electrode, the resistance increased remarkably ($R_{et} \approx 450\ \Omega$) (Fig. S-1A, curve c),

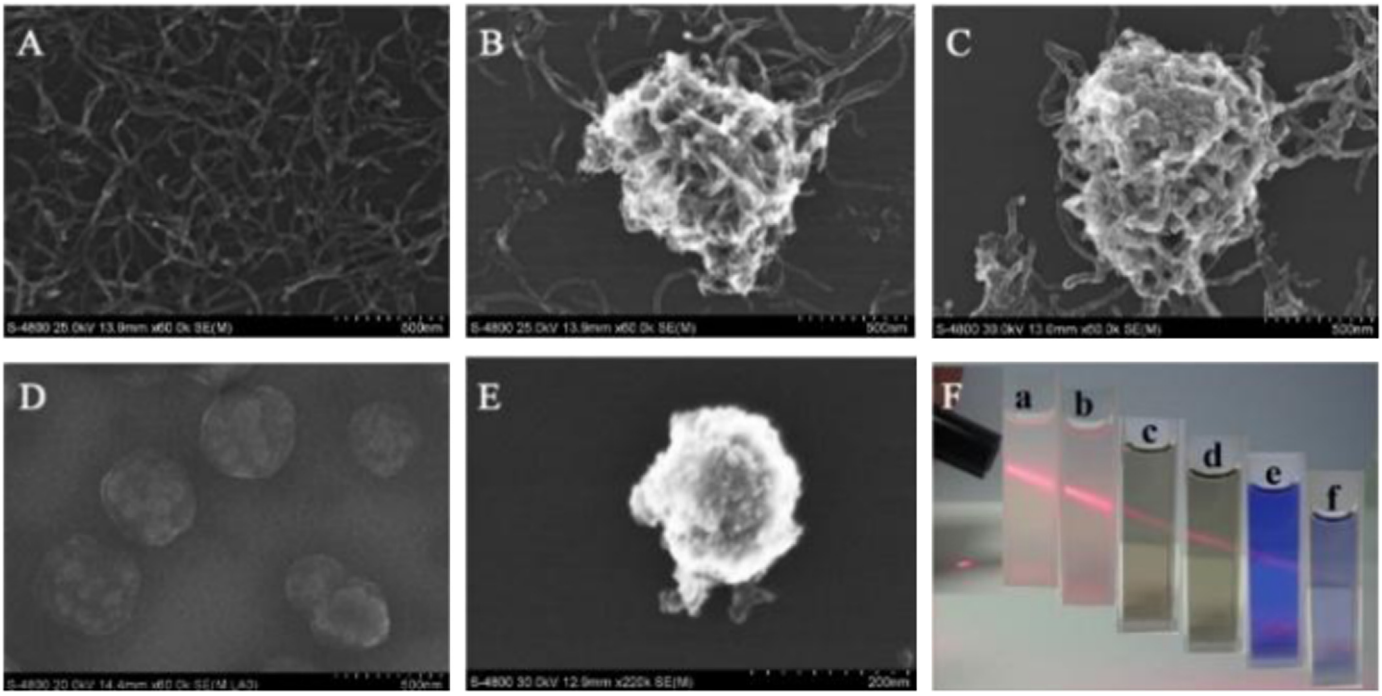


**Fig. 1.** SEM images of (A) MWCNT, (B) MWCNT/PEI, (C) MWCNT /PEI /Thi/AuNPs, (D) $TiO_2$ NPs and (*E*) $TiO_2$ NPs /AuNPs. And the tyndall effect (F) for the solution of (a) $TiO_2$ NPs, (b) $TiO_2$ NPs /AuNPs, (c) MWCNT, (d) MWCNT/PEI, (e) MWCNT/PEI/Thi/AuNPs.

because the DNA with non-electroactive property impeded the electron transfer. Ultimately, when non-conductive HT was modified on the electrode surface, the resistance increased furtherly. ($R_{et} \approx 900\ \Omega$) (curve d). The $R_s$, $R_{et}$, $C_{dl}$ and $Z_w$ of equivalent circuit represented the electrolyte resistance, electronic transfer resistance, double layer capacitance and the Warburg impedance, respectively. In addition, CV was further employed to characterize the electrochemical behaviors of the modified electrode at different stages using the redox probe of $[Fe(CN)_6]^{3-/4-}$. In Fig. S-1B, a well-defined redox peak of $[Fe(CN)_6]^{3-/4-}$ could be observed on the bare electrode (Fig. S-1B, curve a). When AuNPs were deposited on the electrode surface, the redox peak current increased obviously suggesting the good conductivity of AuNPs (Fig. S-1B, curve b). When capture DNA 1 and capture DNA 2 were modified on the electrode surface, an obvious decrease of redox peak current could be observed (Fig. S-1B, curve c), since the DNA could hinder the electron transfer. Finally, after the electrode was blocked with HT, the redox peak current decreased furtherly. (Fig. S-1B, curve d).

### 3.3. The multiplex capability of the fabricated PEC biosensor

The capability of the fabricated PEC biosensor for simultaneous detection of multiplexed genes on single interface was demonstrated in Scheme 1. The incubation of ORVOA 1 gene (2.5 fM) with the biosensor resulted in a 96.2 nA photocurrent response for excitation light source on 590 nm (light 1) while the photocurrent response corresponding to excitation light source on 365 nm (light 2) remained unchanged. Similarly, the presence of p53 gene (2.5 fM) led to a 106.4 nA photocurrent response for the excitation light source on 365 nm, and the photocurrent response corresponding to excitation light source on 590 nm remained unchanged. Then, a double photocurrent response on both 590 nm and 365 nm excitation light sources could be observed when ORVOA 1 gene and p53 gene were incubated on the biosensor. This comparison indicated the fabricated PEC biosensor possessed excellent feasibility for multiplexed detection on single interface.

### 3.4. The photocurrent generation and enhancement mechanisms of the synthesized photoactive nanomaterials

The photocurrent generation and enhancement mechanisms for the MWCNT/PEI/Thi/AuNPs photoactive materials were shown in Fig. 2A. Firstly, under 590 nm excitation light source, the electrons ($e^-$) of MWCNT/PEI conjugates migrated from valence band (VB) to conduction band (CB) (a), then the electrons further migrated to the electrode surface (b). In the presence of nearby molecular Thi as photosensitizer, a largely enhanced photoelectron emission ability of the MWCNT/PEI/Thi nanocomposites could be obtained due to the high molar absorption coefficient of Thi. The electrons of Thi can migrate from highest occupied molecular orbital (HOMO) level to lowest unoccupied molecular orbital (LUMO) level (c), and then the electrons further migrated to the nearby surface of MWCNT/PEI nanocomposites (d). In the presence of AuNPs, the electrons near the Fermi level ($E_f$) states of AuNPs migrated to the surface plasmon (SP) states (e) and further transferred to LUMO level of Thi molecule (f). At the same time, the plasmon energy of AuNPs could be also transferred to the nearby Thi molecule and the MWCNT/PEI nanocomposites (g), helping the separation of electron-hole ($e^-$-$h^+$) pairs of the Thi molecule and MWCNT/PEI nanocomposites, leading to a large enhancement of photocurrent response. The holes on the MWCNT/PEI nanocomposites could drift to the holes of Thi molecule (h) and then the holes on Thi molecule further drifted to the holes of AuNPs (i). With the help of electron donor ($H_2O_2$) in the electrolyte, the $H_2O_2$ could inject electron to the holes of AuNPs which achieved the separation of electrons and holes (j).

In Fig. 2B, according to the plasmonic near-field absorption effects (PRET) of AuNPs, the optical path length of the semiconductor $TiO_2$ NPs could be largely increased by the light scattering from AuNPs, leading to a large enhancement of the photocurrent. Firstly, under the excitation light source of 365 nm, the electrons of $TiO_2$ NPs migrated from VB to CB (a), and then the electrons further migrated to the electrode surface (b). In the presence of the nearby AuNPs, the electrons near the $E_f$ of AuNPs were excited to its SP states (c). Then the excited electrons could migrate to the CB of the nearby semiconductor $TiO_2$ NPs (d). The plasmon energy of the AuNPs could transfer to the $TiO_2$ NPs which was helpful for the separation of $e^-$-$h^+$ pairs of $TiO_2$ NPs (e), leading to a large enhancement of the photocurrent of $TiO_2$ NPs/AuNPs composites. And the holes of $TiO_2$ NPs could drift to the holes of AuNPs left in the electron direct injection process (f). The separation of electrons and holes can be accomplished in the presence of $H_2O_2$ (g).

### 3.5. Optimizations of the PEC biosensor

The photocurrent of the fabricated PEC sensors were related to the amount of cleaved signal probes, which was related to the

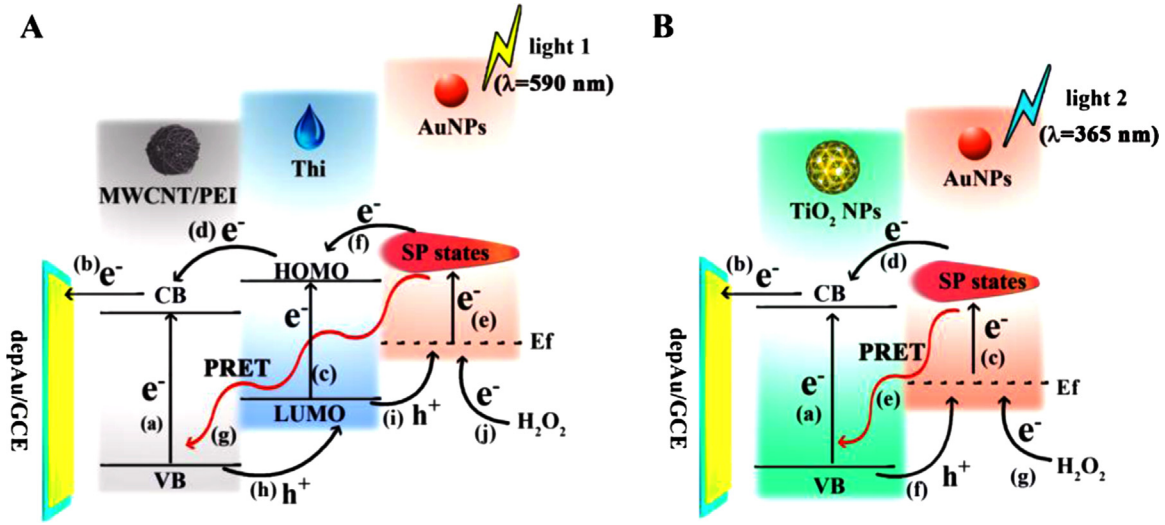


**Fig. 2.** The photocurrent generation and enhancement mechanisms for the MWCNT/PEI/Thi/AuNPs photoactive materials (A) and $TiO_2$ NPs/AuNPs photoactive materials (B).

incubation time of the enzyme-assisted target recycling. With increasing the incubation time, more cleaved signal probes could be obtained for hybridizing with the capture DNA on the fabricated electrode, leading to higher photocurrent response. It could be seen from Figs. S-2A and S-2B, the photocurrent increased obviously with increasing the incubation time and came to maximal value when the incubation time increased to 60 min, which indicated that the optimal incubation time for the enzyme-assisted target recycling strategy was 60 min. Furthermore, the concentration of $H_2O_2$ was estimated to obtain a higher photocurrent response. As shown in Figs. S-2C and S-2D, with increasing concentration of $H_2O_2$, the photocurrent increased obviously and almost leveled off when the concentration of $H_2O_2$ came to 0.1 M, which indicated that the optimal concentration of $H_2O_2$ was 0.1 M in this experiment.

### 3.6. Analytical performance of the PEC biosensor

To estimate the performance of the fabricated PEC biosensor, the targets ORVOA 1 gene and p53 gene with different concentrations were measured by the fabricated PEC biosensor. As shown in Fig. 3, the photocurrent for simultaneous detection of ORVOA 1 gene and p53 gene increased linearly with increasing concentrations of ORVOA 1 gene and p53 gene in the range from 25 aM to 2.5 pM. The linear relationship of ORVOA 1 gene and p53 gene were $I=691.3+39.76$ lg $c_{\text{ORVOA 1 gene}}$ and $I=686.9+39.59$ lg $c_{\text{p53 gene}}$, respectively. Furthermore, the detectable concentrations of p53 gene in the present work were compared with other published works. As shown in Table S-2, our proposed strategy showed a higher sensitivity and a wider linear range, which may be attributed to low background of PEC assay and the novel, integrated signal amplification strategy in this work.

### 3.7. Selectivity of the PEC biosensor

The selectivity of the fabricated PEC biosensor was estimated by incubating the target genes against other different kinds of gene sequences. The interferences including single-base mismatch sequences (smDNA 1, smDNA 2, smDNA 1′, smDNA 2′) and double-base mismatch sequences (dmDNA, dmDNA′). As shown in Fig. 4, the interferences with 100 fold concentration than the targets exhibited no significant current responses compared with that of the targets, indicating a satisfactory selectivity of the proposed PEC biosensor. Besides, all of the relative standard deviations (RSD) to target molecule were lower than 5%, indicating the satisfactory repeatability of the proposed PEC assay.

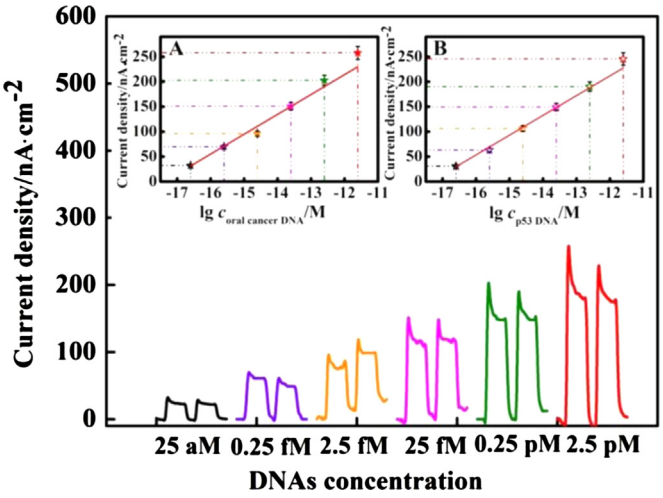


**Fig. 3.** Photocurrent responses for the multiplexed PEC biosensor in the presence of different concentrations of ORVOA 1 gene and p53 gene.

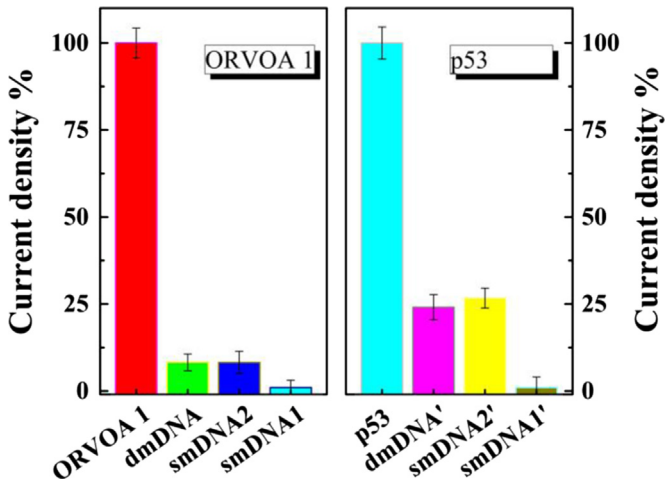


**Fig. 4.** Selectivity evaluation of the proposed PEC biosensor against different mismatched gene sequences.

### 3.8. The applicability of the biosensor for multiplexed evaluation in drug induced cancer cells

The applicability of the fabricated PEC biosensor was evaluated by monitoring the ORVOA 1 gene and p53 gene induced with different concentration of curcumin. Curcumin as a major active component of the food flavoring turmeric is known as a potent anti-tumor agent for some cancer cells. (Prusty and Das 2005) According to the literatures, the ORVOA 1 gene decreased while the p53 gene per Hela cell increased with increasing concentration of curcumin. (Balasubramanyam et al., 2004; Fang et al., 2005) Thus, the concentrations of ORVOA 1 gene and p53 gene in Hela cells can be controlled by adding curcumin with different concentrations (0, 5, 10, 20, 50, 100 μM) to culture medium. As shown in Fig. 5A, the light field microscopy (LF) and fluorescence microscopy (FL) images showed that the amount of Hela cells decreased obviously with increasing the curcumin concentration. The concentration ratio of ORVOA 1 gene and p53 gene per cell were showed in Fig. 5B. The variation trend of these results (Fig. 5C) exhibited that the relative concentration of ORVOA 1 gene in per cell decreased with increasing concentration of curcumin, and the relative concentration of p53 gene per Hela cell increased at the same time, which was identical to the reported literature. (Singh et al., 2013) The evaluation showed a great potential of the fabricated PEC biosensor for multiplexed and ultrasensitive quantification of genes in cell samples for early diagnosis of cancers.

## 4. Conclusions

In summary, a simultaneous PEC assay on single interface was constructed for the first time based on the selectively photoactive materials to monitor multiplexed targets in cells. Contributing to enzyme-assisted target recycling amplification strategy, ultrasensitivity was performed, which made the proposed approach possible to be employed to monitor multiplexed genes per cell. Importantly, the developed PEC assay possessed good applicability for monitoring multiplexed genes with ORVOA 1 gene and p53 gene from Hela cells as models. The ultrasensitive PEC sensing protocol opened up the possibility for detection of genes with ultratrace level, leading to early diagnosis of the particular cancer. Although the concept was demonstrated for dual-analyte sensing, it could be readily expanded for the multiplexed estimation of various kinds of nucleic acid sequences, proteins and cells.

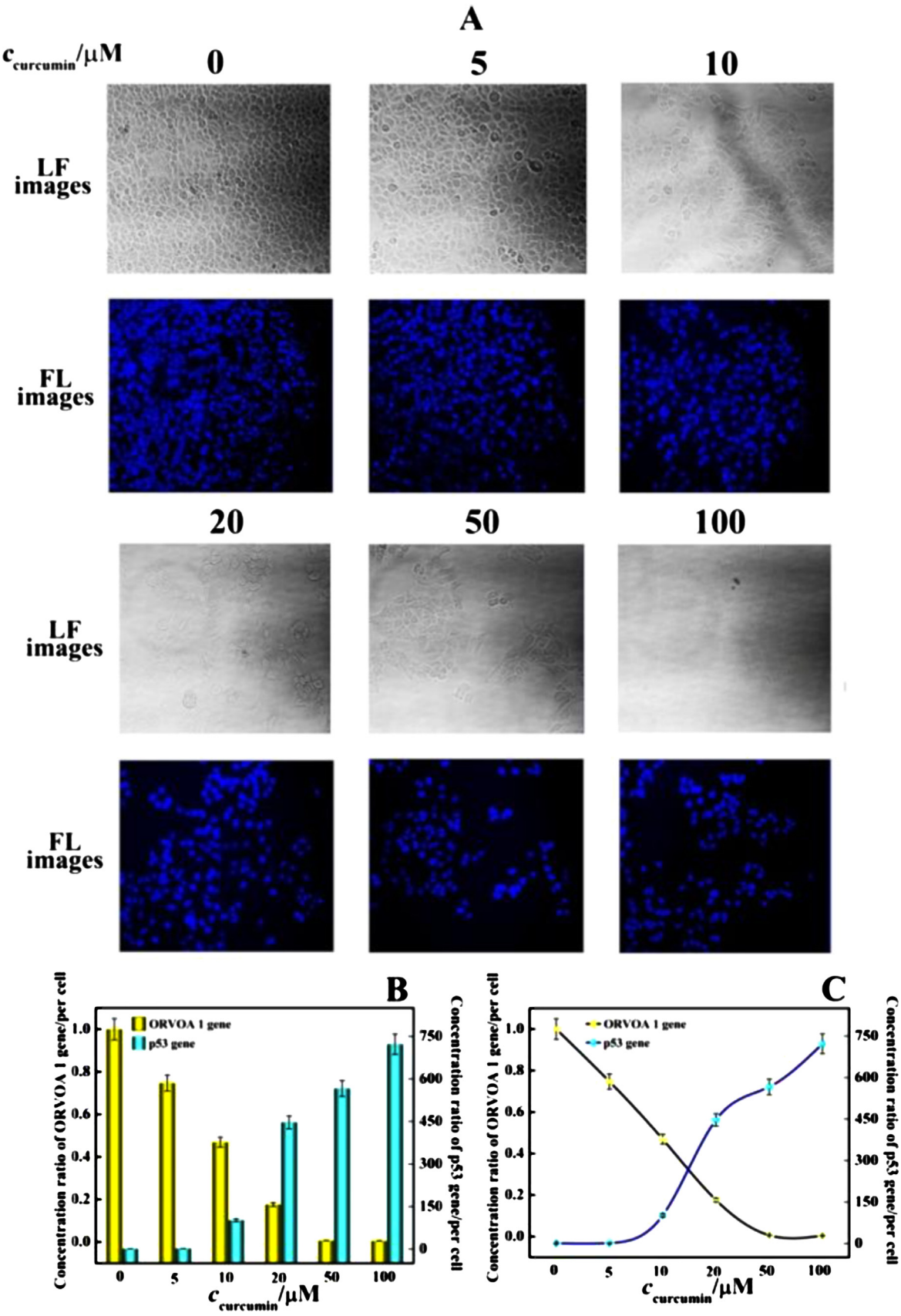


**Fig. 5.** (A) The LF and FL images of curcumin induced Hela cells. (B) The concentration ratio and (C) the variation trend of ORVOA 1 gene and p53 gene in per Hela cell detected by the fabricated PEC.

## Acknowledgements

This work was financially supported by the NNSF of China (21575116, 21275119, 51473136 and 81301518) and the Fundamental Research Funds for the Central Universities (XDJK2015A002), China.

## Appendix A. Supporting information

Supplementary data associated with this article can be found in the online version at http://dx.doi.org/10.1016/j.bios.2016.03.032.

## References

Balasubramanyam, K., Varier, R.A., Altaf, M., Swaminathan, V., Siddappa, N.B., Ranga, U., Kundu, T.K., 2004. J. Biol. Chem. 49, 51163–51178.
Chen, J., Qiu, H.D., Zhang, M.L., Gu, T.N., Shao, S.J., Huang, Y., Zhao, S.L., 2015. Biosens. Bioelectron. 68, 550–555.
Chen, Y., Wang, Q., Xu, J., Xiang, Y., Yuan, R., Chai, Y.Q., 2013. Chem. Commun. 49, 2052–2054.
Fang, J.G., Lu, J., Holmgren, A., 2005. J. Biol. Chem. 280, 25284–25290.
Ge, L., Wang., P.P., Ge, S.G., Li., N.Q., Yu, J.H., Yan., M., Huang, J.D., 2013. Anal. Chem. 85, 3961–3970.
Ge, S.G., Li, W.P., Yan, M., Song, X.R., Yu, J.H., 2015. J. Mater. Chem. B 3, 2426–2432.
Hansen, J.A., Wang, J., Kawde, A.N., Xiang, Y., Gothelf, K.V., Collins, G., 2006. J. Am. Chem. Soc. 128, 2228–2229.
Hu, S.S., Hu, C.G., Liu, Z.H., Wang, J., 2015. Anal. Chem. 87, 9368–9375.
Lee, J.A., Mardyani, S., Hung, A., Rhee, A., Klostranec, J., Mu, Y., Li, D., Chan, W.C., 2007. Adv. Mater. 19, 3113–3118.
Lee-Montiel, F.T., Li, P., Imoukhuede, P.I., 2015. Nanoscale 7, 18504–18514.
Lee, S., Chon, H., Lee, M., Choo, J., Shin, S.Y., Lee, Y.H., Rhyu, I.J., Son, S.W., Oh, C.H., 2009. Biosens. Bioelectron. 24, 2260–2263.
Li, C.L., Wen., K., Mi, T.J., Zhang, X.Y., Zhang., H.Y., Zhang, S.X., Shen, J.Z., Wang, Z.H., 2016. Biosens. Bioelectron. 79, 258–265.
Palecek, E., Bartosik, M., 2012. Chem. Rev. 112, 3427–3481.
Pal, M.K., Rashid, M., Bisht, M., 2015. Biosens. Bioelectron. 73, 146–152.
Pepperkok, R., Squire, A., Geley, S., Bastiaens, P.I.H., 1999. Curr. Biol. 9, 269–272.
Prusty, B.K., Das, B.C., 2005. Int. J. Cancer 113, 951–960.
Singh, S.P., Sharma, M., Gupta, P.K., 2013. Laser Med. Sci. 29, 645–652.
Shen, Q.M., Jiang, J.Y., Liu, S.L., Han, L., Fan, X.H., Fan, M.X., Fan, Q.L., Wang, L.H., Huang, W., 2014. Nanoscale 6, 6315–6321.
Shu, J., Qiu, Z.L., Zhuang, J.Y., Xu, M.D., Tang, D.P., 2015. ACS Appl. Mater. Interfaces 7, 23812–23818.
Wang, W.J., Hao, Q., Wang., W., Bao, L., Lei, J.P., Wang, Q.B., Ju, H.X., 2014. Nanoscale 6, 2710–2717.
Yang, C.Y., Shi, K., Dou, B.T., Xiang, Y., Chai, Y.Q., Yuan, R., 2015. ACS Appl. Mater. Interfaces 7, 1188–1193.
Yuan, L., Tu, W.W., Bao, J.C., Dai, Z.H., 2015. Anal. Chem. 87, 686–692.
Zhao, W.W., Xu, J.J., Chen, H.Y., 2014. Chem. Rev. 114, 7421–7441.
Zhuang, J.Y., Tang, D.Y., Lai, W.Q., Xu, M.D., Tang, D.P., 2015. Anal. Chem. 87, 9473–9480.
Zhu, W.Y., Su, X.P., Gao, X.Y., Dai, Z., Zou, X.Y., 2014. Biosens. Bioelectron. 53, 414–419.